Journal of the Nigerian Association of Mathematical Physics
Volume 26, (*March, 2014*), pp 202 – 219

The Effects of Soot on the Hygroscopicity of Urban Aerosols

B. I. Tijjani and *G.S.M. Galadanci

Department of Physics,
Bayero University, P.M.B. 3011, Kano. NIGERIA.

Abstract

In this paper, the author investigated some microphysical and optical properties of urban aerosols extracted from OPAC by varying the concentrations of soot and determined the effect of hygroscopic growth at the spectral range of 0.25μm to 2.5μm and eight relative humidities (RHs) (0, 50, 70, 80, 90, 95, 98, and 99%).The microphysical properties extracted were radii, volume mix ratio, number mix ratio, mass mix ratio and refractive indices while the optical properties are optical depth and asymmetric parameters all as a function of RHs. Using the microphysical properties, growth factors of the mixtures were determined while using optical depths we determined the enhancement parameters and were then parameterized using some models to determine their relationships with RHs. The data fitted the models very well. The hygroscopicity found using volume mix ratio is found to have higher values. The angstrom coefficients show that the mixtures have bimodal type of distribution with the dominance of fine mode particles and increased with the increase in soot concentrations and RHs.

Keywords: microphysical properties, optical properties, hygroscopic growth, enhancement parameter, spectral range, Angstrom coefficients, bimodal.

1.0 Introduction

The principal source of black carbon is as a result of either fossil fuel combustions or biomass burning except for natural fires, whose sources are small on a global basis. Soot aerosols produced from fossil-fuel combustion, automobile and aircraft emissions and biomass burning are ubiquitous in the atmosphere, comprising10–50% of the total tropospheric particulate matter[1-6]. Once emitted into the atmosphere, soot particles are subjected to several aging processes, including adsorption or condensation of gaseous species [7-9], coagulation with other preexisting aerosols, and oxidation [10-12]. Model calculations have shown that, when associated with other non-absorbing aerosol constituents (e.g., sulfate), soot seems more absorptive and exerts a higher positive direct radiative forcing, and the warming effect by soot nearly balances the net cooling effect of other anthropogenic aerosols[5, 13].

The atmospheric aerosols influence the climate directly by absorbing as well as reflecting the incoming short-wave solar radiation back to spaceor indirectly by acting as cloud-condensation nuclei (CCN) that impact cloud formation and the lifetime and albedo of clouds[4, 6]. Carbonaceous aerosols are considered to be a strong contributor to the indirect effect[14]. Enhanced hydrophilicity associated with soot-aging processes has been experimentally observed, including condensation of gaseous organics[9], H_2SO_4-exposed single carbon microspheres[8], oxidation by OH, O_3, and HNO_3[10-12], or engine combustion[15-17]. Most of the previous studies found relatively small hygroscopic growth of soot below water saturation [i.e., relative humidity (RH) < 100%] on the basis of measured changes in the mobility size, which depends on particle physical dimensions and morphology..Since aerosols are far from being a single component, the question is how relative humidity influences the optical properties of natural aerosol mixtures, which can contain both soluble and insoluble components.

In the natural environment changes in the microphysical and optical properties of the aerosol observed at a given wavelength is a sign that measuring conditions have changed. The changes in these properties can be related either to changes in RH or changes in the aerosol concentrations. Quite often, both factors are present. Optical measurements at one single wavelength will not resolve the question whether the observed change is caused only by the increased humidity or whether the additional aerosol particles have contributed to the changes in these properties. To be able to retrieve more accurate

*Corresponding author: ***G. S. M. Galadanci,*** E-mail: gsmgalad@gmail.com, Tel: +2348037260380 & +2348187492050

information about the aerosol mixtures and RHs, spectral measurements are needed. The more spectral information available, the greater are the chances of getting a more realistic idea of the aerosol composition.Ambient aerosols are external and internal mixtures of particles with different chemical compounds such as soot, sulphate, nitrate, organic carbon and mineral dust. The state of mixing of these components is crucial for understanding the role of aerosol particles in the atmosphere. In recent years, much attention has been paid to the mixing state of soot in aerosols[5, 10], which influences the optical properties and climate effects of aerosols. Also most atmospheric aerosols are externally mixed with respect to hygroscopicity, and consist of more and less hygroscopic sub-fractions [18]. The ratio between these fractions as well as their content of soluble material determines the hygroscopic growth of the overall aerosol. Particle hygroscopicity may vary as a function of time, place, and particle size [18-20].

The interaction of atmospheric aerosol particles with water is a crucial factor affecting their evolution in the atmosphere. By taking up water, particles grow in size and experience modifications to their microphysical and optical properties, which cause the change in their ability to interact with solar radiation.As the ambient relative humidity (RH) changes, hygroscopic atmospheric aerosols undergo phase transformation, droplet growth, and evaporation. Phase transformation from a solid particle to a saline droplet usually occurs spontaneously when the RH reaches a level called the deliquescence humidity. Its value is specific to the chemical composition of the aerosol particle [21, 22]. To model droplet growth, information about water activity and density as a function of solute concentration is needed. Activation into cloud drops is a determining factor in the atmospheric lifetime of particles. Furthermore, cloud droplets and water in deliquesced aerosol particles provide an aqueous medium for chemical reactions, which can lead to a change in the chemical composition of the particles [23-27]. It is well-known that, in the presence of water vapor, the sizes of the aerosols particle may change, depending on the physical and chemical compositionsaerosols[28-31].

The interactions between aerosols and water vapour play a large role in determining their effect on the environment. The chemical and physical characteristics of aerosols are diverse and attempting to encompass such variability within a hygroscopic model is complex. Aerosol may exist in a solid or liquid state or a combination of the two over a wide range of ambient conditions both in the sub and super saturated humid environment [32-35]. Thus, where possible, the ability to couple the chemical and physical characteristics to the equilibrium phase of the aerosol is the ultimate aim of any hygroscopic modeling approach. Atmospheric particles of a defined dry size typically exhibit different growth factors. This is due to either external mixing of particles in an air sample or variable relative fractions of different compounds in individual particles (the latter here in after referred to as quasi-internally mixed)[36].

Most atmospheric aerosols are externally mixed with respect to hygroscopicity, and consist of more and less hygroscopic sub-fractions [18]. The ratio between these fractions as well as their content of soluble material determines the hygroscopic growth of the overall aerosol. Particle hygroscopicity may vary as a function of time, place, and particle size [18-20].

Indeed, the major portion of hygroscopic particle growth is usually related to inorganic species, such as ammonium nitrate, ammonium sulphate, and sodium chloride, whose hygroscopic growth behaviour is known relatively accurately [37, 38]. Also, on the basis of mesoscale model simulations, absorption of solar radiation by internally mixed soot aerosols causes warming in the middle atmosphere and reduction in cloudiness over the tropics [39]. The mixing state and associated physical, optical, and geometrical properties of soot particles are of critical importance in evaluating the effects of light-absorbing aerosols and improving climate predictions by using global climate models (GCMs).Also, on the basis of mesoscale model simulations, absorption of solar radiation by internally mixed soot aerosols causes warming in the middle atmosphere and reduction in cloudiness over the tropics[4].The hygroscopicity of aerosols are currently modeled in global climate models (GCMs), mostly to better predict the scattering properties and size distribution under varying humidity conditions [40] and concentrations. Measured and modeled enhancement factors have been described in several previous studies, including studies on urban [30,41].

A number of previous modeling studies using bulk aerosol models have been performed to estimate the global distribution of carbonaceous aerosols [42-48]. However, these studies must make assumptions about the aerosol size distribution or use empirical relations to predict CDNC from their predicted aerosol mass. Also measured and modeled enhancement factors have been described in several previous studies, including studies on urban[30, 41].

In this paper some microphysical and optical properties of urban aerosols were extracted from OPAC by varying the concentrations of soot at the spectral wavelength of 0.25 to 2.50μm, and relative humidities of 0, 50, 70, 80, 90, 95, 98 and 99%. The microphysical properties extracted are diameters of the aerosols, number mix ratios, volume mix ratio, mass mix ratio and refractive indices. They were used to determine the hygroscopic and the effective refractive indices. One and two parameter models were used to determine the relation between the hygroscopic growths and RHs.The optical properties extracted are optical depth and asymmetric parameters. The optical depth was used to determine the angstrom parameters using power law and enhancement parameters. The angstrom coefficients are used to determine the particles' type and the type mode size distributions. One and two parameter models were used to determine the relationship between the enhancement parameters and hygroscopic growth with RHs and soot concentrations. The asymmetric parameters were used to determine the effects of hygroscopic growth on forward scattering.The aim of this paper is to see how the increase in the concentrations of soot effects the hygroscopic growths, enhancements parameters, mode size distributions and its precisions on the models used.

2.0 Methodology

The models extracted from OPAC are given in Table 1.

Table 1 Compositions of aerosols types [49].

Components	**ModelA (N_i,cm^{-3})**	**ModelB (N_i,cm^{-3})**	**ModelC (N_i,cm^{-3})**
Insoluble	1.50	1.50	1.50
water soluble	35,000.00	35,000.00	35,000.00
Soot	110,000.00	120,000.00	130,000.00
Total	**145,001.50**	**155,001.50**	**165,001.50**

Where (N_i,cm^{-3}) is the number of particles cm^{-3}, water soluble components consist of scattering aerosols, that are hygroscopic in nature, such as sulfates and nitrates present in anthropogenic pollution while water insoluble ,and soot are not soluble in water and therefore the particles are assumed not to grow with increasing relative humidity.

The aerosol's hygroscopic growth factor gf(RH), [18, 50] is defined as:

$$gf(RH) = \frac{D(RH)}{D(RH=0)} \quad (1)$$

where RH is taken for seven values 50%, 70%, 80%, 90%, 95%, 98% and 99%.

But since natural aerosols consist of mixtures of both the soluble and insoluble components, and more and less hygroscopic sub fractions, so information on the hygroscopicity modes was merged into an "over-all" hygroscopic growth factor of the mixture, gf_{mix}(RH), representative for the entire particle population as:

$$gf_{mix}(RH) = (\sum_k x_k gf_k^3)^{1/3} \quad (2)$$

where the summation is performed over all compounds present in the particles and x_k represent their respective volume fractions, using the Zdanovskii-Stokes-Robinson relation(ZSR relation)[51-54]. Solute-solute interactions are neglected in this model and volume additivity is also assumed. The model assumes spherical particles, ideal mixing (i.e. no volume change upon mixing) and independent water uptake of the organic and inorganic components.Equation (2) was also computed using the x_k as the corresponding number fractions [55, 56].

We finally proposed the x_k to represent the mass mix ratio of the individual particles though since mass and volume are proportional, but this will enable us to see the effect of hygroscopic growth on the density of the mixture.The RH dependence ofgf_{mix}(RH) on RHs was parameterized by a one-parameter equation, [57] as:

$$gf_{mix}(a_w) = \left(1 + \kappa \frac{a_w}{1-a_w}\right)^{\frac{1}{3}} \quad (3)$$

Here, a_w is the water activity, which can be replaced by the relative humidity RH, if the Kelvin effect is negligible, as for particles with sizes more relevant for light scattering and absorption. Particle hygroscopicity is a measure that scales the volume of water associated with a unit volume of dry particle [57] and depends on the molar volume and the activity coefficients of the dissolved compounds [58]. The coefficient κ is a simple measure of the particle's hygroscopicity and captures all solute properties (Raoult effect,) that is, it is for the ensemble of the particle which can be defined in terms of the sum of its components. The κ value derived a particle of a given composition may vary, depending upon the size, composition and the RH it is derived at.The following sub-divivsions at 85% RH were made by [59] as: nearly-hydrophobic particles (NH): κ<=0.10 (gf_{mix}<=1.21), less-hygroscopic particles (LH): κ=0.10–0.20 (gf_{mix}=1.21–1.37); more-hygroscopic particles (MH):κ>0.20 (gf_{mix}>1.37).

Humidograms of the ambient aerosols obtained in various atmospheric conditions showed that gf_{mix}(RH) could as well be fitted well with a γ-law [28, 60-63] as

$$gf_{mix}(RH) = \left(1 - \frac{RH}{100}\right)^{\gamma} \quad (4)$$

The bulk hygroscopicity factor B under subsaturation RH conditions was determined using the relation:

$$B = (1 - gf_{mix}^3) ln a_w \quad (5)$$

where a_w is the water activity, which can be replaced by the RH as explained before. The equation can be described as the rate of absorption of water of the bulk mixture as the RH increases.

The impact of hygroscopic growth on the aerosol optical depth is usually described by the enhancement factor $f_\tau(RH, \lambda)$:

$$f_\tau(RH, \lambda) = \frac{\tau(RH,\lambda)}{\tau(RH=0,\lambda)} \quad (6)$$

where RH is taken for seven values 50%, 70%, 80%, 90%, 95%, 98% and 99%.

In general the relationship between $f_\tau(RH, \lambda)$ and RH is nonlinear [64]. In this paper we determined the empirical relations between the enhancement parameter and RH [65] as:

$$f_\tau(RH,\lambda) = \frac{\tau(RH,\lambda)}{\tau(RH_{ref},\lambda)} = \left(\frac{100-RH_{ref}}{100-RH_{high}}\right)^{\gamma} \quad (7)$$

where in our study RH_{ref} was 0%, and RH_{high}values were taken for seven values 50%, 70%, 80%, 90%, 95%, 98% and 99%. The γ known as the humidification factor represents the dependence of aerosol optical depth on RH, which results from changes in the particle size and refractive index upon humidification. The use of γ has the advantage of describing the hygroscopic behavior of aerosols in a linear manner over a broad range of RH values; it also implies that particles are deliquesced [66], a reasonable assumption for this data set due to the high ambient relative humidity during the field study. The γ parameter is dimensionless, and it increases with increasing particle water uptake. From previous studies, typical values of γ for ambient aerosol ranged between 0.1 and 1.5 [66-68].

Two parameters empirical relation was also used [29, 64] as;

$$f_\tau(RH,\lambda) = a\left(1-\frac{RH(\%)}{100}\right)^{b} \quad (8)$$

Equations (7) and (8) were verified at wavelengths 0.25, 0.45, 0.55, 0.70, 1.25, and 2.50μm.

To determine the effect of particles distributions as a result of change in RH and soot concentrations,the Angstrom exponent was determined using the spectral behavior of the aerosol optical depth, with the wavelength of light (λ) was expressed as inverse power law [69]:

$$\tau(\lambda) = \beta\lambda^{-\alpha} \quad (9)$$

The Angstromexponent was obtained as a coefficient of the following regression,

$$ln\tau(\lambda) = -\alpha ln(\lambda) + ln\beta \quad (10)$$

However equation (10) was determined as non-linear(that is the Angstrom exponent itself varies with wavelength), and a more precise empirical relationship between the optical depth and wavelength was obtained with a 2nd-order polynomial [70-80] as:

$$\ln\tau(\lambda)=\alpha_2(\ln\lambda)^2 + \alpha_1\ln\lambda + \ln\beta \quad (11)$$

thenwe proposed the cubic relation to determine the type of mode distribution as:

$$\ln X(\lambda)= \ln\beta + \alpha_1\ln\lambda + \alpha_2(\ln\lambda)^2+ \alpha_3(\ln\lambda)^3 \quad (12)$$

where β, α, α_1, α_2, α_3 are constants that were determined using regression analysis with SPSS16.0.forwondows.

We also determined the exponential dependence of the aerosol optical thickness on relative humidity as done by [64] as;

$$\tau(RH) = Ae^{B(RH/100)} \quad (13)$$

where A and B are constants determined using regression analysis with SPSS 16.0.
We finally determine the effect of hygroscopic growth and change in the concentration of soot on the effective refractive indices of the mixed aerosols using the following formula [81]:

$$\frac{\varepsilon_{eff}-\varepsilon_0}{\varepsilon_{eff}+2\varepsilon_0} = \sum_{i=1}^{3} f_i \frac{\varepsilon_i-\varepsilon_0}{\varepsilon_i+2\varepsilon_0} \quad (14)$$

where f_i and ε_i are the volume fraction and dielectric constant of the i^{th} component and ε_0 is the dielectric constant of the host material.

The relation between dielectrics and refractive indices is

$$m_i = \sqrt{\varepsilon_i} \quad (15)$$

For the case of Lorentz-Lorentz [82, 83], the host material is taken to be vacuum, ε_0 =1.

The computation of equ(14) and (15) was done using the complex functions of Microsoft Excel 2010.

3.0 Results And Discussions

Table 2a: the growth factor of the aerosols using number mix ratio (equation (2))*and Bulk hygroscopicity factor (equation(5))*for *Model A.*

RH(%)	50	70	80	90	95	98	99
gf_{mix}(RH)	1.0669	1.1039	1.1408	1.2223	1.3329	1.5170	1.2617
B	0.1485	0.1231	0.1081	0.0871	0.0702	0.0503	0.0101

Table 2b: the growth factor of the aerosols using number mix ratio (equation (2)) *and Bulk hygroscopicity factor (equation (5))* for *Model B*

RH(%)	50	70	80	90	95	98	99
gf_{mix}(RH)	1.0628	1.0977	1.1327	1.2103	1.3161	1.4933	1.6365
B	0.1389	0.1151	0.1011	0.0814	0.0656	0.0471	0.0340

Table 2c: the growth factor of the aerosols using number mix ratio (equation (2)) *and Bulk hygroscopicity factor (equation (5))* for *Model C*

RH(%)	50	70	80	90	95	98	99
gf_{mix}(RH)	1.0592	1.0923	1.1255	1.1995	1.3010	1.4719	1.6106
B	0.1305	0.1082	0.0950	0.0765	0.0617	0.0442	0.0319

From Tables 2a, 2b and 2c it can be seen that there is a decrease in both gf_{mix}(RH) and B with the increase in the concentrations of soot. It can also be observed the hygroscopic growth has caused increase in gf_{mix}(RH) but decrease in B.

The data from Tables 2a, 2b and 2c were applied for the parameterizations of equations (3) and (4). The results obtained are as follows:

The results of the parameterizations by one parameter of equations (3) and (4) for Model A using number mix ratio are:

k=0.0408, $R2$=0.9470 using equation (3)

γ=-0.1026, $R2$=0.9914 using equation (4)

The results of the parameterizations by one parameter of equations (3) and (4) for Model B using number mix ratio are:

k=0.0381, $R2$=0.9470 using equation(3)

γ=-0.0986, $R2$=0.9902 using equation (4)

The results of the parameterizations by one parameter of equations (3) and (4) for Model C using number mix ratio are:

k=0.0358, $R2$=0.9470 using equation (3)

γ=-0.0949, $R2$=0.9891 using equation (4)

From the observations of R^2 it can be seen that the data fitted the equations very well (equations (3) and (4)). It can also be observed that hygroscopicity of the mixtures (k) and γ using γ-law, all decrease with the increase in the concentrations of soot.

Table 3a: the growth factor of the aerosols using volume mix ratio (equation (2)) *and Bulk hygroscopicity factor (equation (5))*for *Model A*

RH(%)	50	70	80	90	95	98	99
gf_{mix}(RH)	1.1680	1.2667	1.3628	1.5641	1.8141	2.1920	2.4746
B	0.4114	0.3683	0.3417	0.2978	0.2549	0.1926	0.1422

Table 3b: the growth factor of the aerosols using volume mix ratio (equation(2)) *and Bulk hygroscopicity factor (equation (5))* for *Model B.*

RH(%)	50	70	80	90	95	98	99
gf_{mix}(RH)	1.1669	1.2652	1.3613	1.5624	1.8126	2.1907	2.4736
B	0.4081	0.3658	0.3397	0.2965	0.2542	0.1922	0.1421

Table 3c: the growth factor of the aerosols using volume mix ratio (equation (2)) *and Bulk hygroscopicity factor (equation (5))* for *Model C.*

RH(%)	50	70	80	90	95	98	99
gf_{mix}(RH)	1.1657	1.2638	1.3597	1.5607	1.8111	2.1895	2.4725
B	0.4048	0.3633	0.3377	0.2952	0.2534	0.1919	0.1419

From Tables 3a, 3b and 3c it can be seen that there is a decrease in both gf_{mix}(RH) and B with the increase in the concentrations of soot. It can also be observed the hygroscopic growth has caused increased in gf_{mix}(RH) but decrease in B.

The data from Tables 3a, 3b and 3c were applied for the parameterizations of equations (3) and (4). The results obtained are as follows:

The results of the parameterizations by one parameter of equations (3) and (4) for Model A using volume mix ratio are:

k=0.1577, $R2$=0.9612 usingequation (3)
γ=-0.1979, $R2$=0.9997 using equation (4)

The results of the parameterizations by one parameter of equations (3) and (4) for Model B using volume mix ratio are:

k=0.1574, $R2$=0.9615 using equation (3)
γ=-0.1977, $R2$=0.9997 using equation (4)

The results of the parameterizations by one parameter of equations (3) and (4) for Model C using volume mix ratio are:

k=0.1572, $R2$=0.9618 using equation (3)
γ=-0.1975, $R2$=0.9997 using equation (4)

From the observations of R^2 it can be seen that the data fitted the equations very well (equations (3) and (4)). It can also be observed that hygroscopicity of the mixtures (k) and γ using γ-law, all decrease with the increase in the concentrations of soot.

Table 4a: the growth factor of the aerosols using mass mix ratio (equation (2)) *and Bulk hygroscopicity factor (equation (5))*for *Model A.*

RH(%)	50	70	80	90	95	98	99
gf_{mix}(RH)	1.1582	1.2499	1.3407	1.5346	1.7819	2.1618	2.4477
B	0.3837	0.3398	0.3146	0.2754	0.2389	0.1839	0.1373

Table 4b: the growth factor of the aerosols using mass mix ratio (equation (2)) *and Bulk hygroscopicity factor (equation (5))* for *Model B.*

RH(%)	50	70	80	90	95	98	99
gf_{mix}(RH)	1.1575	1.2490	1.3396	1.5333	1.7807	2.1607	2.4468
B	0.3817	0.3382	0.3133	0.2744	0.2383	0.1836	0.1372

Table 4c: the growth factor of the aerosols using mass mix ratio (equation (2)) *and Bulk hygroscopicity factor (equation (5))* for *Model C.*

RH(%)	50	70	80	90	95	98	99
gf_{mix}(RH)	1.1567	1.2480	1.3386	1.5321	1.7794	2.1597	2.4458
B	0.3796	0.3366	0.3121	0.2735	0.2377	0.1833	0.1370

From Tables 4a, 4b and 4c it can be seen that there is a decrease in both gf_{mix}(RH) and B with the increase in the concentrations of soot. It can also be observed the hygroscopic growth has caused increased in gf_{mix}(RH) but decrease in B.

The data from Tables 4a, 4b and 4c were applied for the parametrisations of equations (3) and (4). The results obtained are as follows:

The results of the parameterizations by one parameter of equations (3) and (4) for Model A are:

k=0.1515, $R2$=0.9652 usingequation (3)
γ=-0.1933, $R2$=0.9995 using equation (4)

The results of the parameterizations by one parameter of equations (3) and (4) for Model B are:

k=0.1513, $R2$=0.9654 using equation (3)
γ=-0.1932, $R2$=0.9994 using equation (4)

The results of the parameterizations by one parameter of equations (3) and (4) for Model C are:

k=0.1511, $R2$=0.9655 using equation(3)
γ=-0.1930, $R2$=0.9994 using equation (4)

From the observations of R^2 it can be seen that the data fitted the equations very well (equations (3) and (4)). It can also be observed that hygroscopicity of the mixtures (k) and γ using γ-law, all decrease with the increase in the concentrations of soot.This shows that the addition of soot has caused decrease in the water uptake of the mixture.

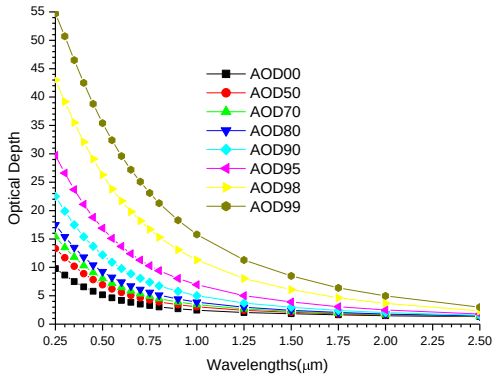

Figure 1a: A graph of optical depth against wavelengths for *Model A*

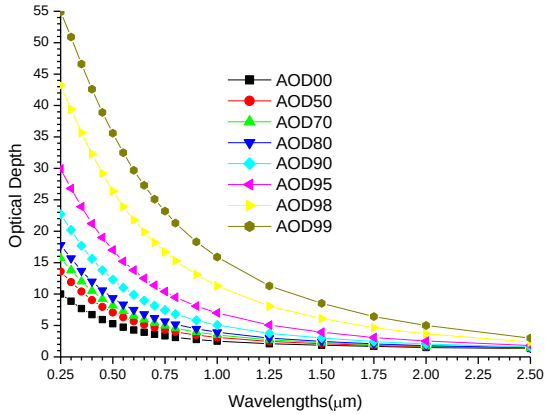

Figure 1b: A graph of optical depth against wavelengths for *Model B.*

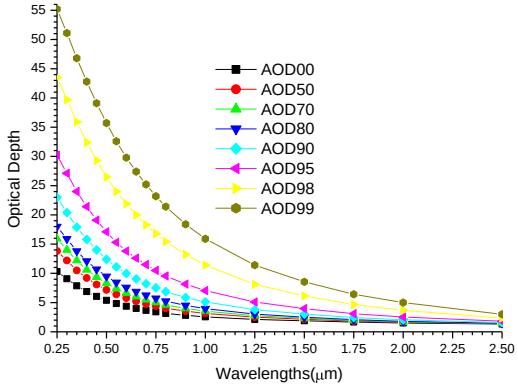

Figure 1c: A graph of optical depth against wavelengths for *Model C.*

From Figures 1a, 1b and 1c, it can be observe that there is a slight increase in optical depth with the increase in RH and the concentrations of soots. The optical depth follows a relatively smooth decrease with wavelength for all RHs and aerosols concentrations and can be approximated with power law wavelength dependence.It is evident from the plots that there is relatively strong wavelength dependence of optical depth at shorter wavelengths that gradually decreases towards longer wavelengths irrespective of the RH and soot concentrations, attributing to the presence of fine to coarse particles. The presence of a higher concentration of the fine-mode particles which are selective scatters enhance the irradiance scattering in shorter wavelength only while the coarse-mode particles provide similar contributions to the AOD at both wavelengths[84]. This also shows that hygroscopic growth has more effect on fine particles than coarse particles. The relation of optical depth with RH is such that at the deliquescence point (90 to 99%) this growth with higher humidities increases substantially, making this process strongly nonlinear with relative humidity [39, 85].

The data that were used in plotting Figures 1a, 1b and 1c were applied to equation (13), at the wavelengths of 0.25, 1.25 and 2.50μm. The results obtained are as follows:

The relation between optical depth and RHs using equation (13) for *Model A* are:

At λ=0.25μ, A=7.5406, B=1.4725, R^2= 0.7044
At λ=1.25 μ, A=1.5067, B=1.3464, R^2= 0.5646
At λ=2.50 μ, A=1.1308, B=0.5675, R^2= 0.4285

The relation between optical depth and RHs using equation(13) for *Model B.* are:

At λ=0.25μ, A=7.7479, B=1.4532, R^2=0.7039
At λ=1.25 μ, A=1.5384, B=1.3308, R^2= 0.5623
At λ=2.50 μ, A=1.1423, B=0.5671, R^2= 0.4347

The relation between optical depth and RHs using equation (13) for *Model C* are:

At λ=0.25μ, A=7.9690, B=1.4323, R^2= 0.6984
At λ=1.25 μ, A=1.5640, B=1.3222, R^2= 0.5602
At λ=2.50 μ, A=1.1593, B=0.5580, R^2=0.4273

The relation between optical depth and RH shows decrease in $R^2$and exponent B with the increase in wavelength and also shows decrease with the increase in the concentrations of soot.However the decrease with the increase in the concentrations of soot demonstrated how the soot acts as a cloud condensation nuclei and this makes the particles to become bigger and this causes the exponents and the relation to decrease just as Angstrom coefficients decrease with the increase in the particle sizes.

Table 5a:the results of the Angstrom coefficients for Model A using equations (10), (11) and (12) at the respective relative humidities using regression analysis with SPSS16 for windows.

RH	Linear		Quadratic			Cubic			
(%)	R2	α	R2	α1	α2	R2	α1	α2	α3
0	0.9898	0.9237	0.9965	-0.8721	0.1125	0.9990	-0.9492	0.2005	0.1154
50	0.9961	1.0500	0.9970	-1.0284	0.0469	0.9996	-1.1182	0.1494	0.1343
70	0.9973	1.1025	0.9973	-1.0994	0.0067	0.9998	-1.1912	0.1115	0.1373
80	0.9972	1.1452	0.9976	-1.1605	-0.0335	0.9999	-1.2510	0.0697	0.1353
90	0.9942	1.2124	0.9984	-1.2663	-0.1173	1.0000	-1.3458	-0.0266	0.1189
95	0.9864	1.2602	0.9993	-1.3583	-0.2135	1.0000	-1.4141	-0.1498	0.0835
98	0.9705	1.2739	0.9999	-1.4250	-0.3289	1.0000	-1.4384	-0.3137	0.0199
99	0.9577	1.2520	0.9998	-1.4309	-0.3893	0.9999	-1.4161	-0.4062	-0.0222

Table 5b:the results of the Angstrom coefficients for Model B using equations (10), (11) and (12) at the respective relative humidities using regression analysis with SPSS16 for windows.

RH	Linear		Quadratic			Cubic			
(%)	R2	α	R2	α1	α2	R2	α1	α2	α3
0	0.9899	0.9296	0.9965	-0.8781	0.1121	0.9990	-0.9560	0.2011	0.1166
50	0.9961	1.0531	0.9970	-1.0313	0.0474	0.9996	-1.1212	0.1499	0.1344
70	0.9973	1.1045	0.9973	-1.1012	0.0073	0.9998	-1.1928	0.1119	0.1371
80	0.9973	1.1465	0.9976	-1.1614	-0.0324	0.9999	-1.2517	0.0706	0.1351
90	0.9943	1.2127	0.9984	-1.2658	-0.1155	1.0000	-1.3455	-0.0246	0.1192
95	0.9866	1.2601	0.9993	-1.3573	-0.2117	1.0000	-1.4134	-0.1477	0.0839
98	0.9708	1.2738	0.9999	-1.4241	-0.3271	1.0000	-1.4378	-0.3114	0.0206
99	0.9580	1.2519	0.9998	-1.4300	-0.3877	0.9999	-1.4155	-0.4042	-0.0217

Table 5c:the results of the Angstrom coefficients for Model C using equations (10), (11) and (12) at the respective relative humidities using regression analysis with SPSS16 for windows.

RH	Linear		Quadratic			Cubic			
(%)	R2	α	R2	α1	α2	R2	α1	α2	α3
0	0.9901	0.9353	0.9965	-0.8840	0.1117	0.9990	-0.9621	0.2009	0.1168
50	0.9961	1.0558	0.9970	-1.0340	0.0474	0.9996	-1.1240	0.1501	0.1346
70	0.9973	1.1064	0.9973	-1.1026	0.0081	0.9998	-1.1944	0.1128	0.1372
80	0.9973	1.1477	0.9976	-1.1621	-0.0314	0.9999	-1.2524	0.0717	0.1351
90	0.9944	1.2130	0.9984	-1.2654	-0.1141	1.0000	-1.3451	-0.0231	0.1193
95	0.9868	1.2599	0.9993	-1.3563	-0.2098	1.0000	-1.4127	-0.1454	0.0844
98	0.9711	1.2735	0.9999	-1.4229	-0.3252	1.0000	-1.4371	-0.3090	0.0212
99	0.9584	1.2519	0.9998	-1.4293	-0.3860	0.9999	-1.4153	-0.4020	-0.0209

First, generally from Tables 5a, 5b and 5c, it can be observed that at each table there is an increase in α with the increase in RH except at 99%RH which is assumed to the delinquent point of the mixtures. As the concentration of soot was increased, the values of α2 decrease at 0% RH, this signifies the increase in the concentrations of fine particles and increase in mode size. However, at RHs 50 to 70% it can be observed that the positive curvatures increase with the increase in soot while at RHs 80 to 99% the negative curvatures decrease and this shows that increase in the concentrations of soot with the increase in RH.Also since the addition of black carbon may not change the effective radius of the mixture because of the its size, but does change the Angstrom coefficient because of its strong absorbing properties, which affect extinction and hence the Angstrom coefficient.The cubic part signifies mode distributions as bi-modal.

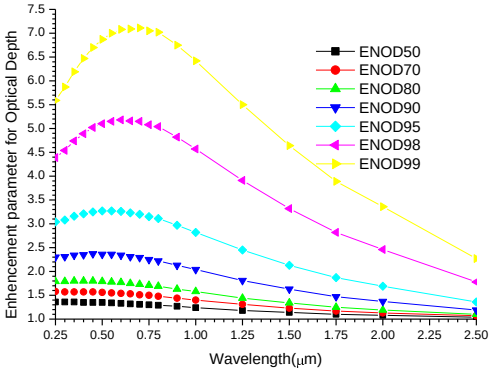

Figure 2a: A graph of enhancement parameter for optical depth against wavelengths for Model A

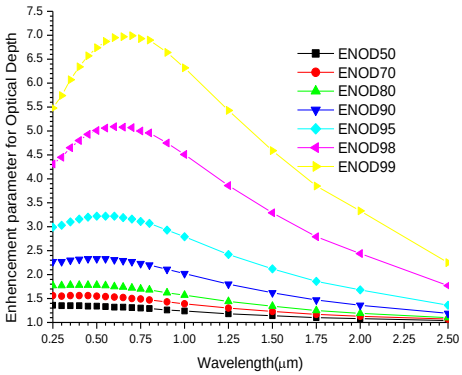

Figure 2b: A graph of enhancement parameter for optical depth against wavelengths for Model B.

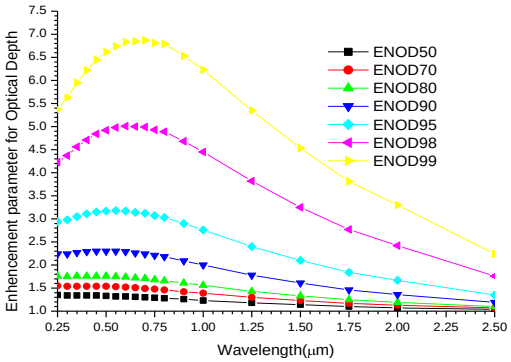

Figure 2c: A graph of enhancement parameter for optical depth against wavelengths for Model C

Figures 2a, 2b and 2c show that the enhancement factors increase with the increase in RH but decrease with the increase in the concentrations of soot in almost non-linear form. A very interesting phenomena is the visible range window(0.4 - 0.7 μm) where the enhancement is higher with the increase in RH but decreases with the increase in the concentrations of soot. This shows that increase in the concentrations of soot causes increase in cloud cover, and/or reflective aerosol and this can lead to increase in global albedo, which can cause the reduction of energy input into Earth-Atmosphere system and finally can cause cooling effect.That is, it does not allow most solar radiation through to the surface and disable solar radiation to "deliver"the bulk of its energy to the surface (for use in climate processes). Also, on the basis of mesoscale model simulations, absorption of solar radiation by internally mixed soot aerosols causes warming in the middle atmosphere and reduction in cloudiness over the tropics [30]. Black carbon is the aerosol that exerts the most complex effect on climate. Like all aerosols, BC scatters a portion of the direct solar beam back to space, which leads to a reduction in solar radiation reaching the surface of the Earth. This reduction is manifest as an increase in solar radiation reflected back to space at the top of the atmosphere, that is, a negative radiative forcing (cooling). A portion of the incoming solar radiation is absorbed by BC-containing particles in the air. This absorption leads to a further reduction in solar radiation reaching the surface. At the surface, the result of this absorption is cooling because solar radiation that would otherwise reach the surface is prevented from doing so. However, the absorption of radiation by BC-containing particles leads to a heating in the atmosphere itself. Thus, absorption by BC leads to a negative radiative forcing at the surface and a positive radiative forcing in the atmosphere. The net effect of BC is to add heat to the atmosphere and decrease radiative heating of the surface.

The data that were used in plotting figures 2a, 2b and 2c were applied for the parametrisations of equations (7) and (8), at the wavelengths of 0.25, 0.45, 0.55, 0.70, 1.25 and 2.50μm. The results obtained are as follows:

The results of the fitted curves of equations (7) and (8) for *Model A* are presented as follows;

For a single parameter using equation (7).

At λ=0.25μ, γ=0.2809, R^2= 0.9974
At λ=0.45μ, γ=1.2907, R^2=0.9828
At λ=0.55 μ, γ=1.3247, R^2=0.9791
At λ=0.70 μ, γ=1.3252, R^2=0.9749
At λ=1.25 μ, γ=0.2113, R^2= 0.9575
At λ=2.50 μ, γ=0.0701, R^2= 0.8914

For two parameters using equation (8).

At λ=0.25μ, a=1.2062, b=-0.2985, R^2=0.9940
At λ=0.45μ, a=1.1550, b=-1.3517, R^2=0.9362
At λ=0.55 μ, a=1.2477, b=-1.4233, R^2=0.9294
At λ=0.70 μ, a=1.3208, b=-1.4517, R^2=0.9212
At λ=1.25 μ, a=2.1526, b=-0.2781, R^2=0.9619
At λ=2.50 μ, a=2.8743, b=-0.1048, R^2=0.9078

The results of the fitted curves of equations (7) and (8) for *Model B* are presented as follows;

For a single parameter using equation (7).

At λ=0.25μ, γ=1.1202, R^2= 0.9897
At λ=0.45μ, γ=1.2684, R^2= 0.9832
At λ=0.55 μ, γ=1.3030, R^2= 0.9795
At λ=0.70 μ, γ=1.3053, R^2= 0.9754
At λ=1.25 μ, γ=1.0163, R^2= 0.9740
At λ=2.50 μ, γ=0.5040, R^2= 0.9432

For two parameters using equation (8).

At λ=0.25μ, a=0.8161, b=-1.0531, R^2= 0.9550
At λ=0.45μ, a=1.1355, b=-1.3210, R^2= 0.9362
At λ=0.55 μ, a=1.2287, b=-1.3928, R^2= 0.9294
At λ=0.70 μ, a=1.3023, b=-1.4230, R^2= 0.9214
At λ=1.25 μ, a=1.1104, b=-1.0508, R^2= 0.9012
At λ=2.50 μ, a=0.1056, b=-0.2958, R^2= 0.8795

The results of the fitted curves of equations (7) and (8) for *Model C* are presented as follows;

For a single parameter using equation (7).

At λ=0.25μ, γ=1.1004, R^2= 0.9896
At λ=0.45μ, γ=1.2472, R^2=0.9835
At λ=0.55 μ, γ=1.2822, R^2=0.9799
At λ=0.70 μ, γ=1.2857, R^2=0.9759
At λ=1.25 μ, γ=1.0045, R^2= 0.9744
At λ=2.50 μ, γ=0.5018, R^2= 0.9424

For two parameters using equation (8).

At λ=0.25μ, a=0.7975, b=-1.0276 , R^2= 0.9549
At λ=0.45μ, a=1.1158, b=-1.2916, R^2=0.9362
At λ=0.55 μ, a=1.2100, b=-1.3637, R^2=0.9294
At λ=0.70 μ, a=1.2842, b=-1.3950, R^2=0.9214
At λ=1.25 μ, a=1.0923, b=-1.0331 , R^2= 0.9013
At λ=2.50μ, a=0.1013, b=-0.2922, R^2= 0.8797

For one and two parameters, the exponents increase as the wavelength is increased from ultra violet to solar spectral window (0.25– 0.7μm) and has maximum value at 0.7μm. The increase in the concentration soot causes the exponents to fluctuateat uvand near infrared, but decrease at the solar spectral window (0.4–0.7μm).

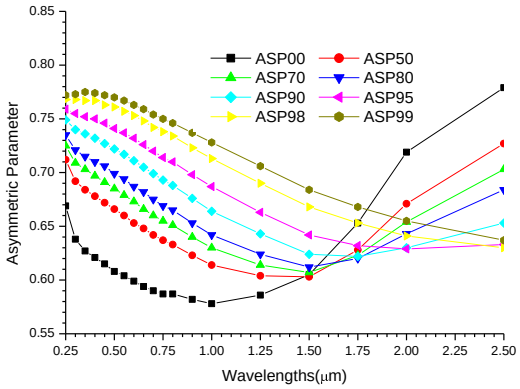

Figure 3a: A graph of Asymmetric parameter against wavelengths for Model A

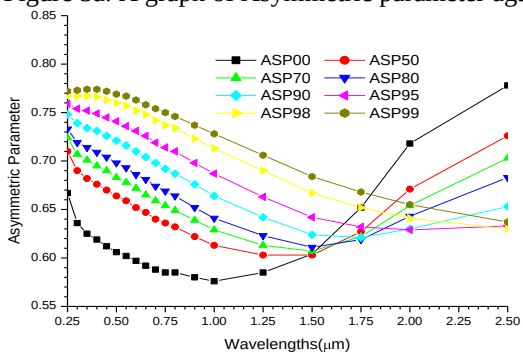

Figure 3b: A graph of Asymmetric parameter against wavelengths for Model B.

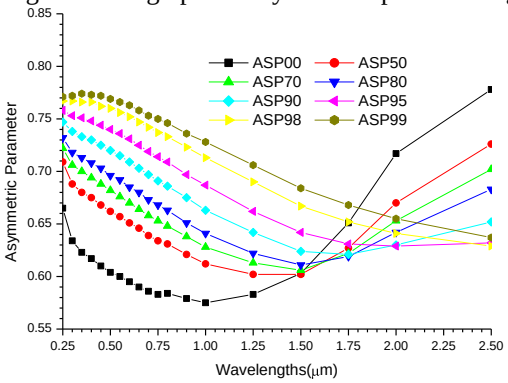

Figure 3c: A graph of Asymmetric parameter against wavelengths for Model C

Figures 3a, 3b and 3c show a slight decrease of the asymmetric parameter with the increase in soot concentrations. As from uv to near infrared (0.25-1.5μm) the increase in RH enhances forward scattering, but as from1.5 to 2.5μm which is part of far infrared, the forward scattering decreases with the increase in RH.

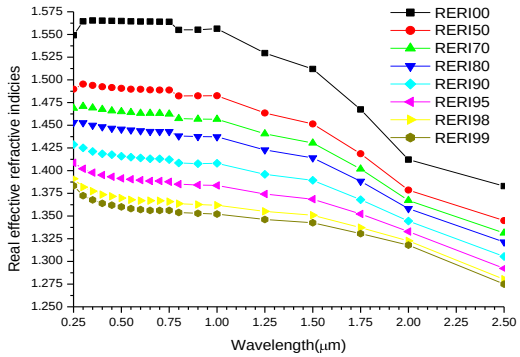

Figure 4a: A plot of real effective refractive indices against wavelength for Model A.

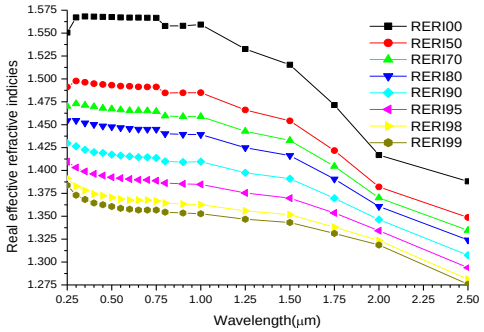

Figure 4b: A plot of real effective refractive indices against wavelength for Model B.

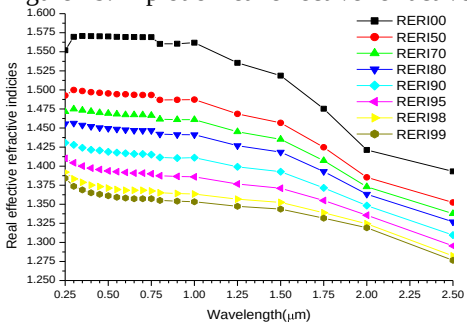

Figure 4c: A plot of real effective refractive indices against wavelength for Model C

Figures 4a, 4b and 4c show an increase in the effective real refractive indices with the increase in the soot concentrations. With respect to RH, at 0% RH at the visible spectral wavelength, the plots are in a straight line. This shows the dominance of spherical particles at 0% RH, but as the RH increases, the plots changed to non-linear, and this shows the increase in the dominance of non-spherical particles with the increase in RHs.

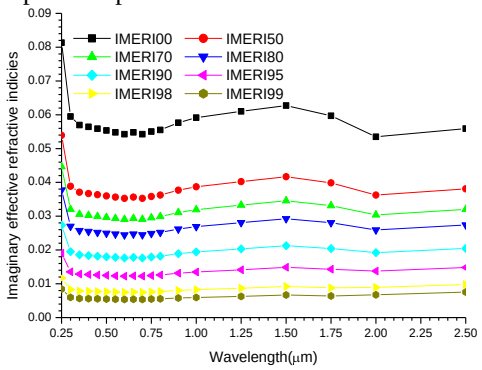

Figure 5a: A plot of imaginary effective refractive indices against wavelength using volume mix ratio for Model A.

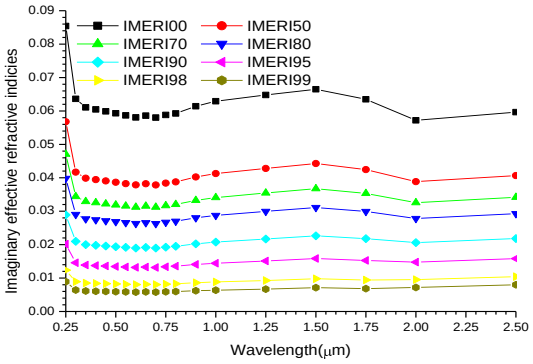

Figure 5b: A plot of imaginary effective refractive indices against wavelength using volume mix ratio for Model B.

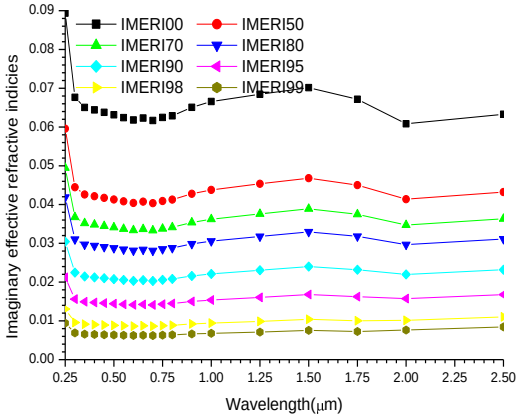

Figure 5c: A plot of imaginary effective refractive indices against wavelength using volume mix ratio for Model C

Figures 5a, 5b, and 5c show increase in the effective imaginary refractive indices with the increase in the soot concentrations but decreases with the increase in RH. As the RH increases the relation between the effective refractive indices and wavelength is becoming more linear.

4.0 Conclusions

In this paper we investigated the influence of relative humidity and soot on the microphysical and optical properties of atmospheric aerosol mixtures. The principal conclusions are:

1) Equation (3) with mass mix ratios has higher R2 while equation (4) has higher values of R2 using volume mix ratio. But since volume mix ratios gave higher values of $gf_{mix}(RH)$, k and γ, and the values of R2 are greater than 95%, it can be concluded that just as the optical effects of atmospheric aerosols are more closely related to their volume than their number [86, 87], we discovered that the microphysical properties are also more closely related to their volume followed by mass. The decrease in the values of $gf_{mix}(RH)$, k and γ with the increase in soot concentration show that soot concentrations decreases hygroscopicity of aerosols.

2) Changes in RH and soot concentrations modified the optical properties not only of hygroscopic aerosol mixtures but also of mixtures containing non-hygroscopic aerosols like black carbon. As a result of wetting the hydroscopic particles grow, thereby changing the effective radius of the aerosol mixture and subsequently the aerosol extinction or aerosol optical thickness[88]. The changes are more substantial especially at the delinquent points where the hygroscopic growth factor, optical parameters and enhancement parameters increase so substantial that the process become strongly nonlinear with relative humidity [39, 85, 88]. This effect is observed at different wavelengths, but for higher RH, the increase in AOT values is more evident at smaller wavelengths than longer wavelengths. The importance of determining $gf_{mix}(RH)$ as a function of RH and volume fractions, mass fractions and number fractions, and enhancement parameters as a function of RH and wavelengths can be potentially important because it can be used for efficiently representing aerosols-water interactions in global models.

3) The observed variations in Angstrom coefficients can be explained by changes in the effective radius of a mixture resulting from changes in RH and/or soot concentrations: the larger the number of small aerosol particles, the smaller the effective radius and the larger the Angstrom coefficient.As a consequence of non-uniform increase in the optical depth with the increase in RH, the Ångströmcoefficient also becomes a function of RH, though at the delinquent points it decreases with the increase in RHs.This is because at the delinquent conditions the hygroscopic aerosols particles grow and this is what makes the Angstrom coefficients to decrease.However, the change in Angstrom coefficient due to variation in RH is more than that caused by differences in soot concentrations.

4) The effect of RHs on asymmetric parameter shows that for smaller particles the hygroscopic growth increase forward scattering while for coarse particle it decreases forward scattering.It shows that increase in RH increases forward scattering because particle growth enhances forward diffraction [89]for smaller particles while in larger particles it causes increase in the backward scattering. It also shows that the mixture is internally mixed for smaller particles because of the increase in forward scattering as a result of the hygroscopic growth [90].

5) These hygroscopic growth behaviors also reveal an immense potential of light scattering enhancement in the forward direction at high humidities and the potential for being highly effective cloud condensation nuclei for smaller particles.

6) Finally, the data fitted our models very and can be used to extrapolate the hygroscopic growth and enhancements parameters at any RH. The values of R2 from the models show that Kelvin effects can be neglected.

Model Answers

1.	B	2.	B	3.	A	4.	D	5.	A	6.	E	7.	A	8.	B	9.	Bonus	10.	Bonus
11.	E	12.	A	13.	D	14.	C	15.	D	16.	C	17.	E	18.	B	19.	A	20.	D
21.	A	22.	B	23.	E	24.	C	25.	BONUS										

References

[1]IPCC (2007)Intergovernmental Climate Change Reporteds Solomon S,*etal*.(Cambridge Univ Press, Cambridge, UK). http://www.ipcc.ch/ipccreports/ar4-wg1.htm.

[2]Penner J. E., Eddleman H., Novakov T. (1993).Towards the development of a global inventory for black carbon emissions.Atmos Environ A27:1277–1295.

[3]Chameides W. L., Bergin M. (2002). Climate change: Soot takes center stage.Science 297:2214 –2215.

[4]Ackerman A. S., et al. (2000). Reduction of tropical cloudiness by soot.Science288:1042–1047.

[5]Jacobson M. Z. (2001). Strong radiative heating due to the mixing state of blackcarbon in atmospheric aerosols.Nature409:695– 697.

[6] McMurry P. H., Shepherd M, Vickery J (2004). Particulate Matter Science for Policy Makers: A NARSTO Assessment(Cambridge Univ. Press, Cambridge, UK).

[7] Zhang D.and Zhang R. (2005). Laboratory investigation of heterogeneous interaction of sulfuric acid with soot.EnvironSci Technol39:5722–5728.

[8] Wyslouzil B. E., et al. (1994). Observation of hydration of single, modified carbon aerosols.Geophys Res Lett21:2107–2110.

[9] Saathoff H., et al. (2003). Coating of soot and $(NH_4)_2SO_4$particles by ozonolysis products of alpha-pinene.J Aerosol Sci. 34:1297–1321.

[10] ZuberiB.,et al., (2005). Hydrophilic properties of aged soot.Geophys Res Lett32, L01807, doi:10.1029/2004GL021496.

[11] Kotzick R. andNiessner R. (1999).The effects of aging processes on critical supersaturation ratios of ultrafine carbon aerosols.Atmos Environ33:2669 –2677.

[12] Kotzick R., PanneU., and Niessner R. (1997). Changes in condensation properties of ultrafine carbon particles subjected to oxidation by ozone.J Aerosol Sci28:725–735.

[13] Jacobson M. Z. (2000). A physically-based treatment of elemental carbon optics: Implications for global direct forcing of aerosols.Geophys Res Lett27:217–220.

[14] Novakov, T. andPenner, J. E. (1993). Large Contribution of Organic Aerosols to Cloud-Condensation-Nuclei Concentrations, Nature, 365, 823–826, ISI:A1993MD95100045.

[15] Popovitcheva O. B., Trukhin M. E., Persiantseva N. M.andShonija N. K. (2001).Water adsorption on aircraft-combustor soot under young plume conditions.Atmos Environ35:1673–1676.

[16] Gysel M., et al. (2003). Properties of jet engine combustion particles during the PartEmis experiment: Hygroscopic growth at supersaturated conditions.Geophys Res Lett30, doi:10.1029/2003GL017294.

[17] Weingartner E., Burtscher H. and Baltensperger U. (1997). Hygroscopic properties of carbon and diesel soot particles.Atmos Environ31:2311–2327.

[18] Swietlicki, E., Hansson, H.-C., H¨ameri, K., Svenningsson, B., Massling, A., et al.: Hygroscopic properties of submicrometer atmospheric aerosol particles measured with H-TDMA instruments in various environments – a review, Tellus B, 60(3), 432–469, 2008.

[19] McMurry, P. and Stolzenburg, M.: On the sensitivity of particle size to relative humidity for Los Angeles aerosols, Atmos. Environ., 23, 497–507, 1989.

[20] Cocker, D., Whitlock, N., Flagan, R., and Seinfeld, J. H.: Hygroscopic properties of Pasadena, California aerosol, Aerosol Sci. Technol, 35, 2, 637–647, 2001.

[21] Orr Jr. C., Hurd F. K., Corbett W. J., 1958, Aerosol size and relative humidity, J. Colloid Sci., 13, 472–482.

[22] Tang I. N., 1976, Phase transformation and growth of aerosol particles composed of mixed salts, J. Aerosol Sci., 7, 361–371.

[23] Hegg, D. A.: The importance of liquid phase oxidation of SO2 in the atmosphere, J. Geophys. Res., 90, 3773–3779, doi:10.1029/JD090iD02p03773, 1985.

[24] Blando, J. D. and Turpin, B. J.: Secondary organic aerosol formation in cloud and fog droplets: a literature evaluation of plausibility, Atmos. Environ., 34, 1623–1632, doi:10.1016/S1352-2310(99)00392-1, 2000.

[25] El Haddad, I., Yao Liu, Nieto-Gligorovski, L., Michaud, V., Temime-Roussel, B., Quivet, E., Marchand, N., Sellegri, K., and Monod, A.: In-cloud processes of methacrolein under simulated conditions – Part 2: Formation of secondary organic aerosol, Atmos. Chem. Phys., 9, 5107–5117, doi:10.5194/acp-9-5107-2009, 2009.

[26] Bateman, A. P., Nizkorodov, S. A., Laskin, J., and Laskin, A.: Photolytic processing of secondary organic aerosols dissolved in cloud droplets, Phys. Chem. Chem. Phys., 13, 12199–12212, doi:10.1039/c1cp20526a, 2011.
[27] Ervens, B., Turpin, B. J., and Weber, R. J.: Secondary organic aerosol formation in cloud droplets and aqueous particles (aqSOA): a review of laboratory, field and model studies, Atmos. Chem. Phys., 11, 11069–11102, doi:10.5194/acp-11-11069-2011, 2011.
[28] Kasten, F. (1969): Visibility forecast in the phase of pre-condensation, Tellus, XXI, 5, 631–635.
[29] Hanel, G. (1976). The Properties of Atmospheric Aerosol Particles as Functions of Relative Humidity at Thermodynamic Equilibrium with Surrounding Moist Air.InAdvances in Geophysics, Vol. 19 , H. E. Landsberg and J. Van Mieghem, eds., Academic Press, New York, pp. 73–188.
[30] Fitzgerald, J. W., Hoppel, W. A., and Vietti, M. A.(1982): The size and scattering coefficient of urban aerosol particles at Washington, DC as a function of relative humidity, J. Atmos. Sci., 39, 1838–1852.
[31] Ogren, J. A. and Charlson R. J.: Implications for models and measurements of chemical inhomogeneities among cloud droplets, Tellus, 44B, 489–504, 1992.
[32] Corrigan, C. E. and Novakov, T.: Cloud condensation nucleus activity of organic compounds: a laboratory study, Atmos. Environ., 33 (17), 2661–2668, 1999.
[33] Pitchford, M. L. and Mcmurry, P. H. (1994): Relationship between Measured Water-Vapor Growth and Chemistry of Atmospheric Aerosol for Grand-Canyon, Arizona, in Winter 1990, Atmos. Environ., 28 (5), 827–839.
[34] Shulman, M. L., Jacobson, M. C., Charlson, R. J., Synovec, R. E., and Young, T. E.: Dissolution behavior and surface tension effects of organic compounds in nucleating cloud droplets (vol. 23, p. 277, 1996), Geophys. Res. Lett., 23 (5), 603–603, 1996.
[35] Swietlicki, E., Zhou, J. C., Berg, O. H., Martinsson, B. G., Frank, G., Cederfelt, S. I., Dusek, U., Berner, A., Birmili, W., Wiedensohler, A., Yuskiewicz, B., and Bower, K. N.: A closure study of sub-micrometer aerosol particle hygroscopic behaviour, Atmos. Res., 50 (3-4), 205–240, 1999.
[36] Buzorius, G., Zelenyuk, A., Brechtel, F., and Imre, D.: Simul-taneous determination of individual ambient particle size, hy-groscopicity and composition. Geophys. Res. Lett., 29, 1974, doi:10.1029/2001GL014221, 2002.
[37] Tang, I.N. and Munkelwitz, H.R. (1994). Water Activities, Densities, and Refractive Indices of Aqueous Sulfates and Sodium Nitrate Droplets of Atmospheric Importance. J. Geophys. Res.99: 18801–18808.
[38] Brechtel, F. J., and S. M. Kreidenweis (2000), Predicting particle criticalsupersaturation from hygroscopic growth measurements in the humidified TDMA. Part II: Laboratory and ambient studies, J. Atmos. Sci., 57 , 1872-1887.
[39] Fitzgerald , J. W. (1975) Approximation formulas for the equilibrium size of an aerosol particle as a function of its dry size and composition and ambient relative humidity. J. Appl .Meteorol. , 14, 1044 –1049.
[40] Randall, D. A., Wood, R. A., Bony, S., Colman, R., Fichefet, T., Fyfe, J., Kattsov, V., Pitman, A., Shukla, J., Srinivasan, J., Stouf-fer, R. J., Sumi, A., and Taylor, K. E.: Contribution of Working Group I to the Fourth Assessment Report of the Intergovernmen-tal Panel on Climate Change – Climate Models and their Evalua-tion, Cambridge University Press, Cambridge, United Kingdom and New York, 589–662, 2007.
[41] Yan, P., Pan, X. L., Tang, J., Zhou, X. J., Zhang, R. J., and Zeng, L. M.: Hygroscopic growth of aerosol scattering coeffi-cient: a comparative analysis between urban and suburban sites at winter in Beijing, Particuology, 7, 52–60, 2009.
[42] Chung, S. H. and Seinfeld, J. H. (2002).Global distribution and climate forcing of carbonaceous aerosols, J. Geophys. Res. Atmos., 107, ISI:000180860300016.
[43] Cooke, W. F., Liousse, C., Cachier, H., and Feichter, J.: Construction of a 1 degrees × 1 degrees fossil fuel emission data set for carbonaceous aerosol and implementation and radiative impact in the ECHAM4 model, J. Geophys. Res.-Atmos., 104, 22 137–22 162, ISI:000082789200006, 1999.
[44] Cooke, W. F. and Wilson, J. J. N.: A global black carbon aerosol model, J. Geophys. Res.-Atmos., 101, 19 395–19 409, ISI:A1996VE25800041, 1996.
[45] Liousse, C., Penner, J. E., Chuang, C., Walton, J. J., Eddleman, H., and Cachier, H. A.(1996).Global three-dimensional model study of carbonaceous aerosols, J. Geophys. Res.Atmos., 101, 19 411–19 432, ISI:A1996VE25800042.
[46] Lohmann, U., Feichter, J., Penner, J., and Leaitch, R. (2000). Indirect effect of sulfate and carbonaceous aerosols: A mechanistic treatment, J. Geophys. Res. Atmos., 105, 12 193–12 206, ISI:000087366600008.
[47] Penner, J. E., Chuang, C. C., and Grant, K. (1998). Climate forcing by carbonaceous and sulfate aerosols, Clim. Dynamm., 14, 839–851, ISI:000076963400001.
[48] Reddy, M. S. and Boucher, O. (2004).A study of the global cycle of carbonaceous aerosols in the LMDZT general circulation model, J. Geophys. Res. Atmos., 109, ISI:000222916300002.
[49] Hess M., Koepke P., and Schult I (May 1998), Optical Properties of Aerosols and Clouds: The Software Package OPAC, Bulletin of the A merican Met. Soc. 79, 5, p831-844.
[50] Randles , C. A. , Russell L. M. and. Ramaswamy V. (2004) Hygroscopic and optical properties of organic sea salt aerosol and consequences for climate forcing, Geophysical Research Letters, Vol. 31, L16108, doi:10.1029/2004GL020628.

[51] Sjogren, S., Gysel, M., Weingartner, E., Baltensperger, U., Cubi-son, M. J., Coe, H., Zardini, A. A., Marcolli, C., Krieger, U. K., and Peter, T.: Hygroscopic growth and water uptake kinetics of two-phase aerosol particles consisting of ammonium sulfate, adipic and humic acid mixtures, J. Aerosol Sci., 38, 157–171, doi:10.1016/j.jaerosci.2006.11.005, 2007.

[52] Stokes, R. H. and Robinson, R. A.: Interactions in aqueous nonelec-trolyte solutions. I. Solute-solvent equilibria, J. Phys. Chem., 70, 2126–2130, 1966.

[53] Meyer, N. K., Duplissy, J., Gysel, M., Metzger, A., Dommen, J., Weingartner, E., Alfarra, M. R., Prevot, A. S. H., Fletcher, C., Good, N., McFiggans, G., Jonsson,˚ A. M., Hallquist, M., Baltensperger, U., and Ristovski, Z. D.: Analysis of the hy-groscopic and volatile properties of ammonium sulphate seeded and unseeded SOA particles, Atmos. Chem. Phys., 9, 721–732, doi:10.5194/acp-9-721-2009, 2009.

[54] Stock M., Y. F. Cheng, W. Birmili, A. Massling, B. Wehner, T. Muller, S. Leinert, N. Kalivitis,N. Mihalopoulos, and A. Wiedensohler, Hygroscopic properties of atmospheric aerosol particles over the Eastern Mediterranean: implications for regional direct radiative forcing under clean and polluted conditions, Atmos. Chem. Phys., 11, 4251–4271, 2011 www.atmos-chem-phys.net/11/4251/2011/ doi:10.5194/acp-11-4251-2011.

[55] Duplissy J., P. F. DeCarlo, J. Dommen, M. R. Alfarra, A. Metzger, I. Barmpadimos, A. S. H. Prevot, E. Weingartner, T. Tritscher, M. Gysel, A. C. Aiken, J. L. Jimenez, M. R. Canagaratna , D. R. Worsnop, D. R. Collins, J. Tomlinson, and U. Baltensperger, (2011) Relating hygroscopicity and composition of organic aerosol particulate matter Atmos. Chem. Phys., 11, 1155–1165, www.atmos-chem-phys.net/11/1155/2011/ doi:10.5194/acp-11-1155-2011.

[56] Meier J., B. Wehner, A. Massling,*, W. Birmili, A. Nowak, T. Gnauk, E. Br¨ uggemann, H. Herrmann, H. Min, and A. Wiedensohler Hygroscopic growth of urban aerosol particles in Beijing (China) during wintertime: a comparison of three experimental methods, Atmos. Chem. Phys., 9, 6865–6880, 2009 www.atmos-chem-phys.net/9/6865/2009/

[57] Petters, M. D. and Kreidenweis, S. M. (2007).A single parameter representation of hygroscopic growth and cloud condensation nucleus activity. Atmos. Chem. Phys. 7(8): 1961–1971.

[58] Christensen, S. I. and Petters, M. D. (2012).Th e role of temperature in cloud droplet activation. J. Phys. Chem. A 116(39): 9706–9717.

[59] Liu P. F., Zhao C. S., Gobel T., Hallbauer E., Nowak A., Ran L., Xu W. Y., Deng Z. Z., Ma N., Mildenberger K., Henning S., Stratmann F., and Wiedensohler A. (2011) Hygroscopic proper ties of aerosol par ticles at high relative humidity and their diurnal variations in the Nor th China Plain, Atmos. Chem. Phys. Discuss., 11, 2991–3040

[60] Swietlicki, E., Zhou, J., Covert, D. S., H¨ameri, K., Busch, B., V¨akeva, M., Dusek, U., Berg, O. H., Wiedensohler, A., Aalto, P., M¨akel¨a, J., Martinsson, B. G., Papaspiropoulos, G., Mentes, B., Frank, G., and Stratmann, F.: Hygroscopic properties of aerosol particles in the northeastern Atlantic during ACE-2, Tellus, 52B, 201–227, 2000.

[61] Birmili, W., Nowak, A., Schwirn, K., Lehmann, K.et al. (2004) A new method to accurately relate dry and humidified number size distributions of atmospheric aerosols. Journal of Aerosol Science 1, 15–16, Abstracts of EAC, Budapest 2004.

[62] Gysel, M., McFiggans, G. B., and Coe, H.: Inversion of tandem differential mobility analyser (TDMA) measurements, J. Aerosol Sci., 40, 134–151, 2009.

[63] Putaud, J. P. (2012): Interactive comment on "Aerosol hygroscopicity at Ispra EMEP-GAW station" by M. Adam et. al., Atmos. Chem. Phys. Discuss., 12, C1316–C1322.

[64] Jeong M. J, Li Z., Andrews E., Tsay S. C., (2007) Effect of aerosol humidification on the column aerosol optical thickness over the Atmospheric Radiation Measurement Southern Great Plains site, J. Geophys. Res., 112, D10202, doi:10.1029/2006JD007176.

[65] Doherty, et al., 2005. A comparison and summary of aerosol optical properties as observed in situ from aircraft, ship, and land during ACE-Asia. Journal of Geophysical Research 110, D04201.

[66] Quinn, P. K., et al. (2005) , Impact of particulate organic matter on the relative humidity dependence of light scattering: A simplified parameterization, Geophys. Res. Lett., 32, L22809, doi:10.1029/2005GL024322.

[67] Gasso S., et al. (2000), Influence of humidity on the aerosol scattering coefficient and its effect on the upwelling radiance during ACE-2, Tellus, Ser. B , 52, 546 – 567.

[68] Clarke, A., et al. (2007), Biomass burning and pollution aerosol over North America: Organic components an d their influence on spectral optical properties and humidification response, J. Geophys. Res., 11 2, D12S18, doi:10.1029/2006JD007777.

[69] Angstrom, A.(1961): Techniques of Determining the Turbidity of the At-mosphere, Tellus, 13, 214–223.

[70] King, M. D. and Byrne, D. M.: A method for inferring total ozone content from spectral variation of total optical depth obtained with a solar radiometer, J. Atmos. Sci., 33, 2242–2251, 1976.

[71] Eck, T. F., Holben, B. N., Reid, J. S., Dubovic, O., Smirnov, A., O'Neil, N. T., Slutsker, I., and Kinne, S.: Wavelength dependence of the optical depth of biomass burning, urban, and desert dust aerosols, J. Geophys. Res., 104(D24), 31 333–31 349, 1999.

[72] Eck, T. F., Holben, B. N., Dubovic, O., Smirnov, A., Slutsker, I., Lobert, J. M., and Ramanathan, V.: Column-integrated aerosol optical properties over the Maldives during the northeast mon-soon for 1998–2000, J. Geophys. Res., 106, 28 555–28 566, 2001a.

[73] Eck, T. F., Holben, B. N., Ward, D. E., Dubovic, O., Reid, J. S., Smirnov, A., Mukelabai, M. M., Hsu, N. C., O' Neil, N. T., and Slutsker, I.: Characterization of the optical properties of biomass burning aerosols in Zambia during the 1997 ZIBBEE field campaign, J. Geophys. Res., 106(D4), 3425–3448, 2001b.

[74] Kaufman, Y. J., Aerosol optical thickness and atmospheric path radiance, J. Geophys.Res., 98, 2677-2992, 1993.

[75] O'Neill, N. T., Dubovic, O., and Eck, T. F.(2001): Modified˚ Angstr¨ om exponent for the characterization of submicrometer aerosols, Appl. Opt., 40(15), 2368–2375.

[76] O'Neill, N. T., Eck, T. F., Smirnov, A., Holben, B. N., and Thulasiraman, S.: Spectral discrimination of coarse and fine mode optical depth, J. Geophys. Res., 198(D17), 4559, doi:101029/2002JD002975, 2003.

[77] Pedros, R., Martinez-Lozano, J. A., Utrillas, M. P., Gomez-Amo, J. L., and Tena, F.(2003): Column-integrated aerosol, optical properties from ground-based spectroradiometer measurements at Barrax (Spain) during the Digital Airborne Imaging Spectrometer Experiment (DAISEX) campaigns, J. Geophys. Res., 108(D18), 4571, doi:10.1029/2002JD003331.

[78] Kaskaoutis, D. G. and Kambezidis, H. D.(2006): Investigation on the wavelength dependence of the aerosol optical depth in the Athens area, Q. J. R. Meteorol. Soc., 132, 2217–2234.

[79] Martinez-Lozano, J.A., Utrillas, M.P., Tena, F., Pedros, R., Canada, J., Bosca, J.V., Lorente, J., (2001). Aerosol optical characteristics from summer campaign in an urban coastal Mediterranean area. IEEE Transactions on Geoscience and Remote Sensing 39, 1573–1585.

[80] Schmid, B., Hegg, D.A., Wang, J., Bates, D., Redemann, J., Russell, P.B., Livingston, J.M., Jonsson, H.H., Welton, E.J., Seinfeld, J.H., Flagan, R.C., Covert, D.S., Dubovik, O., Jefferson, A., (2003). Column closure studies of lower tropospheric aerosol and water vapor during ACE-Asia using airborne Sun photometer and airborne in situ and ship-based lidar measurements. Journal of Geophysical Research 108 (D23), 8656.

[81] Aspens D. E. (1982), Local-field effect and effective medium theory: A microscopic perspective Am. J. Phys. 50, 704-709.

[82] Lorentz, H. A. (1880). Ueber die Beziehung zwischen der Fortpflanzungsgeschwindigkeit des Lichtes und der Korperdichte. Ann. P hys. Chem. 9, 641–665.

[83] Lorenz, L. (1880). Ueber die Refractionconstante. A nn. P hys. Chem. 11, 70–103.

[84] Schuster, G.L., Dubovik, O. andHolben, B.N. (2006). Angstrom Exponent and Bimodla Aerosol Size Distributions. J. Geophy. Res. 111: 7207.

[85] Tang I.N.,(1996) Chemical and size effects of hygroscopic aerosols on light scattering coefficient, J. Geophys. Res., 101(D14),19245–19250.

[86] Whitby, K. (1978), The physical characteristics of sulfur aerosols, Atmos. Environ., 12, 135–159.

[87] Seinfeld, J., and S. Pandis (1998), Atmospheric Chemistry and Physics: From Air Pollution to Climate Change, Wiley.

[88] Kuśmierczyk-Michulec, J. (2009). Ångström coefficient as an indicator of the atmospheric aerosol type for a well-mixed atmospheric boundary layer: Part 1: Model development. Oceanologia , Vol. 51, p. 5-39.

[89] Liou, K. N. (2002), An Introduction ro Atmospheric Radiation, 583pp., Elsevier, New York.

[90] Wang, J., and S. T. Martin (2007), Satellite characterization of urban aerosols: Importance of including hygroscopicity and mixing state in the retrieval algorithms, J. Geophys. Res., 112 , D 17203, doi:1 0.1029 /2006JD008078.